Review TRENDS in Cell Biology Vol.15 No.4 April 2005

Cytokinesis series

The stress and strain of cytokinesis

Elizabeth M. Reichl[1,*], Janet C. Effler[1,2,*] and Douglas N. Robinson[1]

[1]Department of Cell Biology, Johns Hopkins University School of Medicine, 725 N. Wolfe St., Baltimore, MD 21205, USA
[2]Department of Electrical and Computer Engineering, Johns Hopkins University, 3400 N. Charles Street, Baltimore, MD 21218, USA

The ultimate goal of all signaling pathways in cytokinesis is to control the mechanical separation of the mother cell into two daughter cells. Because of the intrinsic mechanical nature of cytokinesis, it is essential to understand fully how cell shapes and the material properties of the cell are generated, how these shapes and material properties create force, and how motor proteins such as myosin-II modify the system to achieve successful cytokinesis. In this review (which is part of the *Cytokinesis* series), we discuss the relevant physical properties of cells, how these properties are measured and the basic models that are used to understand cell mechanics. Finally, we present our current understanding of how cytokinesis mechanics work.

Introduction

Cytokinesis, the mechanical separation of a mother cell into two daughter cells, occurs through a series of stereotypical shape changes [1]. Initially, in animal cells the mother cell rounds up and then elongates. The cleavage furrow constricts until a cylindrical bridge forms in the middle of the cell. Finally, the bridge thins and severs, separating the mother cell into two daughter cells.

The regulation of cellular shape plays an important role in cytokinesis and in several fundamental cellular processes, including nuclear organization, gene expression, protein synthesis and cytoskeletal organization [2–4]. Because the control of cell shape is demonstrated exquisitely by a dividing cell, our current understanding of how the cell drives the shape changes of cytokinesis is explored here. The mechanical properties of cells, molecules involved in establishing mechanical properties, experimental techniques for studying cellular mechanics, and models relevant for understanding cytokinesis are discussed. Understanding cellular mechanics provides insight into cytokinesis as well as several other essential cellular processes.

Relevant mechanical components of dividing cells

The physical properties of cells are generated largely by the actin cytoskeleton. Physical properties such as force, viscoelasticity and stretch modulus (see Glossary) are generated by motor proteins, cytoskeletal polymers and associated proteins. In fact, many of the proteins involved in cytokinesis regulate these physical properties. Therefore, understanding these properties and how they are generated and regulated biochemically is necessary to develop an accurate picture of how cytokinesis works.

The stereotypical shape changes of the dividing cell are formed, in part, from material properties that generate passive forces. Passive forces include a Laplace pressure ($P \sim S_c/R$, where P is pressure, S_c is stretch modulus and R is radius), which favors energetically a minimal surface area:volume ratio (Figure 1a). Similar to the surface tension that maintains the spherical shape of a liquid droplet and drives the breakup of a cylindrical thread of a viscoelastic fluid [5,6], the cell contains a cortical actin layer that generates the majority of the cortical stretch modulus [7]. The stretch modulus is an energy cost for deforming the cell that is determined by the in-plane viscoelasticity of the cortex (Figure 1b). Without the actin network, the Laplace pressure derived from the

Glossary

Cortical actin layer: The network of actin filaments and associated cross-linking proteins that are tethered to the plasma membrane.
Bending modulus: A material property that reflects the pressure required to bend a material.
Elasticity: The proportionality constant that relates deformation to applied force (Hooke's Law).
Force: The three types of force (F) involved are inertial (mass×acceleration), viscous (viscous drag×velocity) and elastic (spring constant×displacement). Inertial forces are negligible at the cellular and molecular levels.
Laplace pressure: The pressure generated at a curved, fluid surface. This is generated by the surface stretch modulus and the mean curvature of the fluid, and minimizes the surface area:volume ratio.
Loss (dissipative) modulus: The viscous component of a viscoelastic fluid. It resists movement and causes a loss (dissipation) of energy.
Passive forces: Material forces that are generated from the stretch modulus and the geometry (curvature) of the viscoelastic fluid. Passive forces create pressures (stresses) that can be orders-of-magnitude larger than those generated by molecular motors.
Phase angle: The relationship between elastic and viscous components of a viscoelastic material. The phase angle is the delay between stress application and material deformation. An elastic solid deforms immediately whereas a viscous fluid deforms after a time delay.
Pressure: Force per unit area.
Storage modulus: The elastic component of a viscoelastic fluid. It resists movement but stores energy.
Stress: The pressure applied to a material.
Stretch modulus: The stretch modulus is generated by the in-plane (parallel to the surface) viscoelasticity of the cell.
Viscous drag: The proportionality constant that relates the velocity achieved by a particle immersed in a viscous fluid to a force acting on the particle.
Viscoelasticity: Materials that have dynamic molecular interactions behave viscoelastically. The rate of deformation determines how a material behaves; the material has a high resistance (i.e. elastic) if the material is deformed rapidly, but low resistance (i.e. viscous) if the rate of deformation is slow. This is illustrated by the comparison between floating in a swimming pool (slow deformation) and performing a belly flop into the swimming pool (fast deformation). The resistance offered on different time-scales by the same pool of water makes one think again before performing another belly flop. For more information, see [63,64].

Corresponding author: Robinson, D.N. (dnr@jhmi.edu).
* Elizabeth M. Reichl and Janet C. Effler contributed equally to this review.
Available online 5 March 2005

 0962-8924/$ - see front matter doi:10.1016/j.tcb.2005.02.004

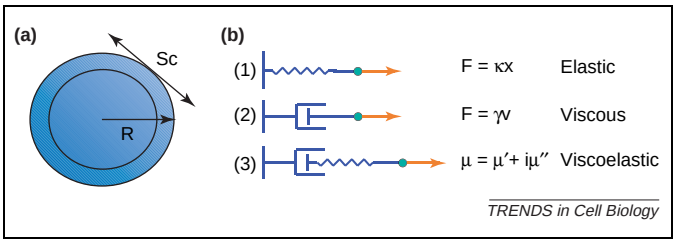

Figure 1. Mechanical properties of cells. **(a)** The cortical stretch modulus (S_c) and the geometry (R, radius) of the cell specify a Laplace pressure. **(b)** 1. Elasticity, which is depicted as a spring of stiffness κ, stores energy when force (F) is applied. Displacement is x. 2. Viscous drag (γ), the fluid resistance to movement, is depicted as a dashpot and results in a loss of energy (dissipation) when force (F) is applied. Velocity is v. 3. Viscoelasticity (μ), which is depicted as a combination of a spring and dashpot, forms a time-scale-dependent complex element that consists of an elastic (storage) modulus, μ′, and a viscous (loss) modulus, μ″.

membrane alone is predicted to be around one order-of-magnitude less than for wild-type cells. Although these material forces are referred to as passive, they are derived from cellular proteins. Thus, the cell expends energy generating these passive material properties. The amounts of myosin-II that are observed to be sent to the cleavage furrow cortex agree closely with those predicted from the stretch modulus, cell geometry and myosin-II mechanochemistry [8]. Thus, the stretch modulus appears to be a reasonable predictor of myosin-II flux through the cleavage furrow cortex.

The viscoelastic character of biological materials determines how much force is required to deform the material. Proteins and networks have a stiffness that is somewhat analogous to a spring. From Hooke's Law, a spring's stiffness (κ) determines the amount of force required to deform it (Figure 1b). Pure actin networks generate relatively low resistance, but cross-linked actin networks can generate extremely high resistances [9–12]. Thus, the spring analogy must be modified to include the dynamic nature of the network (Figure 1b). The viscoelasticity of cross-linked networks is time-scale-dependent because of the association and dissociation rates of the cross-linkers. There are numerous types of actin cross-linkers in the cell cortex, so it is, perhaps, surprising that removal of any single type of crosslinker has quantifiable effects on the mechanical properties of the cell. In fact, by varying the concentration of actin polymers and the ratio of cross-links:actin, the viscoelasticity of the network can vary over three orders-of-magnitude *in vitro* [13]. *In vivo*, cortical viscoelasticity varies by over one order-of-magnitude, ranging from latrunculin treatment to genetic manipulation of specific proteins [7]. Thus, *in vivo*, it appears that the acceptable dynamic range for viability is much narrower than that which is possible for the actin cytoskeletal network *in vitro*.

Viscosity is the energy cost for the bulk flow of a fluid (Figure 1b). The cytoplasmic fluid is a viscoelastic network that is made up of cytoskeletal polymers and organelles. Thus, the resistance of the cytoplasm to deformation is dependent on the applied force, particle size and time-scale [14]. However, for our view of cytokinesis mechanics, the cytoplasm is simplified to a viscous fluid. The largest viscosity is most relevant for the shape changes of cytokinesis because the cell undergoes large-scale changes in shape that require movement of all the cytoplasmic components.

Measuring cortical mechanics

Cellular mechanics have been studied using several techniques, including micropipette aspiration (MPA), laser-tracking microrheology (LTM), atomic force microscopy (AFM), needle poking, laminar flow, magnetic twisting cytometry and agar overlay [7,14–23]. Because each method measures different mechanical properties, it is essential to understand what is being measured to properly interpret the data. Three techniques (MPA, LTM, and AFM), which are used currently in cytokinesis research and which illustrate different mechanical properties of the cell cortex, are discussed (Figure 2). It should be pointed out that cell mechanics are particularly sensitive to actin-filament density as well as crosslinker concentration and kinetics [13]. Furthermore, the networks might have distinct properties depending on whether the cortex is either stretched (stretch modulus) or bent (bending modulus). For *Dictyostelium*, the published value for bending energy (B) is 2×10^{-3} nN μm [19] and for stretch modulus is 1.5 nN μm^{-1} [16,17]. Because bending energy scales as length^{-3} and stretch modulus scales as length^{-1}, the stretch modulus is predicted to dominate on length scales $> \sim 40$ nm $[(B/S_c)^{1/2}]$. Therefore, the stretch modulus is the more important cortical mechanical parameter that governs cytokinesis dynamics over micrometer-scale distances. This might prove to be a general feature, at least for cell types that do not have cell walls.

MPA

MPA has a long history in the cytokinesis literature and is one of the first techniques that was used to micromanipulate cells, introduce mechanical force and measure mechanical properties [17,23–26]. In this assay, a micropipette is placed next to the cell and suction pressure is applied until a stable, hemispherical cap is formed, which defines an equilibrium pressure (Figure 2a). At this equilibrium pressure, the steady-state stretch modulus of the cell can be calculated $[\Delta P = 2S_c(1/R_p - 1/R_c)$ where R_p is the radius of the pipette and R_c is the radius of the cell] [15,27]. Because micropipette radii are typically in the low micrometer range and the cell is deformed over several micrometers, it is reasonable to assume that MPA detects relatively large-scale mechanics.

MPA was used in early studies to show that the cortical stretch modulus of dividing echinoderm eggs varies spatially [24–26]. In some species of echinoderms, the stretch modulus of the entire cortex increases before any furrow formation; however, in all echinoderms, the stretch modulus of the furrow region rises above the polar cortex levels, although sometimes only weakly.

AFM

In AFM, a calibrated cantilever tip is used to probe the surface of a material (Figure 2b). The cantilever position (height) is controlled precisely by a piezo device and deflects as it is lowered onto a surface. For soft materials such as the cell surface, the tip also indents the surface. Because the cantilever deflection is monitored precisely by

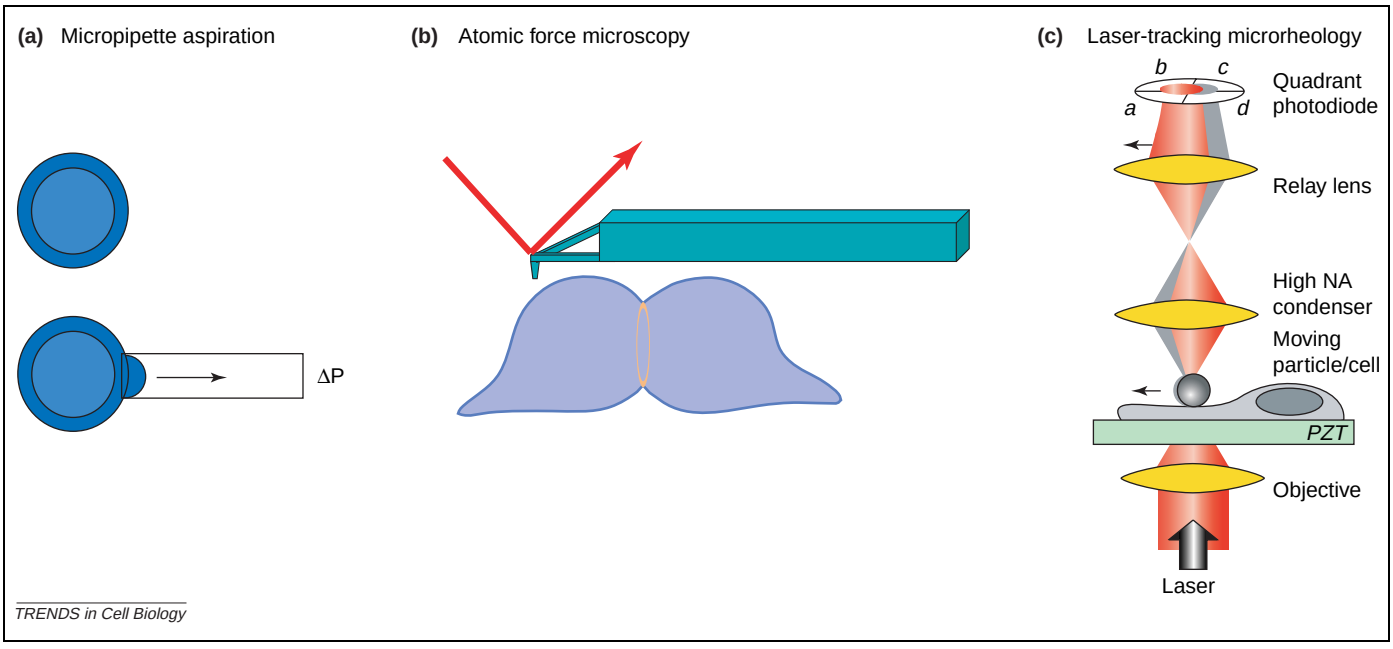

Figure 2. Techniques used in cytokinesis research. **(a)** In MPA, a pipette with a diameter of a few micrometers is placed adjacent to a cell and negative pressure (ΔP) applied to draw the cell into the pipette. **(b)** In AFM, a calibrated cantilever probes the surface of a cell. The cantilever deflection is monitored by a laser, which is recorded by a photodiode detector. **(c)** LTM uses a carboxylated polystyrene bead (micrometer diameter) that attaches non-specifically to the cell surface. As the bead undergoes Brownian motion, its excursion deflects a low-powered laser, which is relayed through a high numerical aperture (NA) condenser and relay lens to a quadrant photodiode detector (with quadrants a–d) and recorded. [Part (c) adapted, with permission, from Ref. [7]].

a laser and photodiode detector, and the height of the cantilever is controlled precisely by the piezo device, the size of the indentation is measured. The bending modulus of the cell's surface is calculated from the measured deflection, cantilever stiffness and contact angle of the tip.

Using AFM in mammalian cells, the bending modulus of the whole cell cortex is observed to increase about fourfold before furrowing [21]. The furrow region increases further just before furrow formation and continues to rise throughout furrow invagination, achieving up to 10-fold above the levels of the global polar cortex. This rise in bending modulus of the cleavage-furrow region is reminiscent of the rise of stretch modulus that is observed with MPA [24–26].

LTM

LTM is just beginning to be incorporated into cytokinesis studies [7]. The strength of this assay is that it allows time-resolved mechanical information to be obtained non-invasively from cells [28–30]. In this assay, a micrometer-size carboxylated polystyrene bead is allowed to settle on the surface of a cell to serve as a noninvasive probe of its mechanical environment (Figure 2c). Brownian motions of the bead are tracked using a low-powered laser, which is deflected by the bead's excursions and relayed to a quadrant photodiode detector. A bead in a softer environment moves more compared with a bead in a stiffer environment. From the bead's movement, the viscoelastic moduli ($\mu = \mu' + i\mu''$, where μ' is the storage modulus and μ'' is the loss modulus) and the mechanical phase angle [$\delta = \tan^{-1}(\mu''/\mu')$] are extracted. The phase angle reflects the liquid-like to solid-like nature of the material. For a pure liquid, the phase angle is 90°, and for a pure elastic solid, the phase angle is 0°. Because the beads are small, they probe local mechanics and because x- and y- excursions are monitored, the in-plane cortical viscoelasticity of the cortex is measured. By LTM, actin-crosslinking proteins such as dynacortin and cortexillin, which control the dynamics of cytokinesis, have significant effects on the stretch modulus [7].

Models of cellular mechanics

To understand cell shape, it is necessary to understand the mechanics of cells. Three broad classes of models, including tensegrity, the cytoskeleton as a soft glassy material and the cortical shell–liquid core model, have emerged to assist in understanding cell mechanics. The tensegrity hypothesis proposes that a balance of compression, tension and adhesion elements govern cellular mechanics [31,32]. Typically, actin filaments and intermediate filaments are considered to be under tension whereas microtubules are under compression. The cytoskeleton has been described as behaving as a soft glassy material, existing close to a glass transition between more rigid and more flexible states [33,34]. Soft glassy behavior is characterized by viscoelasticity that relates to frequency (reciprocal of time), according to a power law. This power-law behavior may arise from having sufficient different actin crosslinkers that are characterized by distinct structural and kinetic properties so that on any time-scale there is a characteristic relaxation time. Whereas tensegrity and soft glassy behavior might, ultimately, need to be considered, the cortical shell–liquid core model has been developed to incorporate many of the relevant physical and molecular parameters for cytokinesis [8,15].

The cortical shell–liquid core model is a continuum model, which simplifies the cell as a cortical shell that is composed of membrane, actin cytoskeleton and associated cross-linking proteins, and a liquid core that consists of viscous cytoplasm [15]. The continuum assumption is

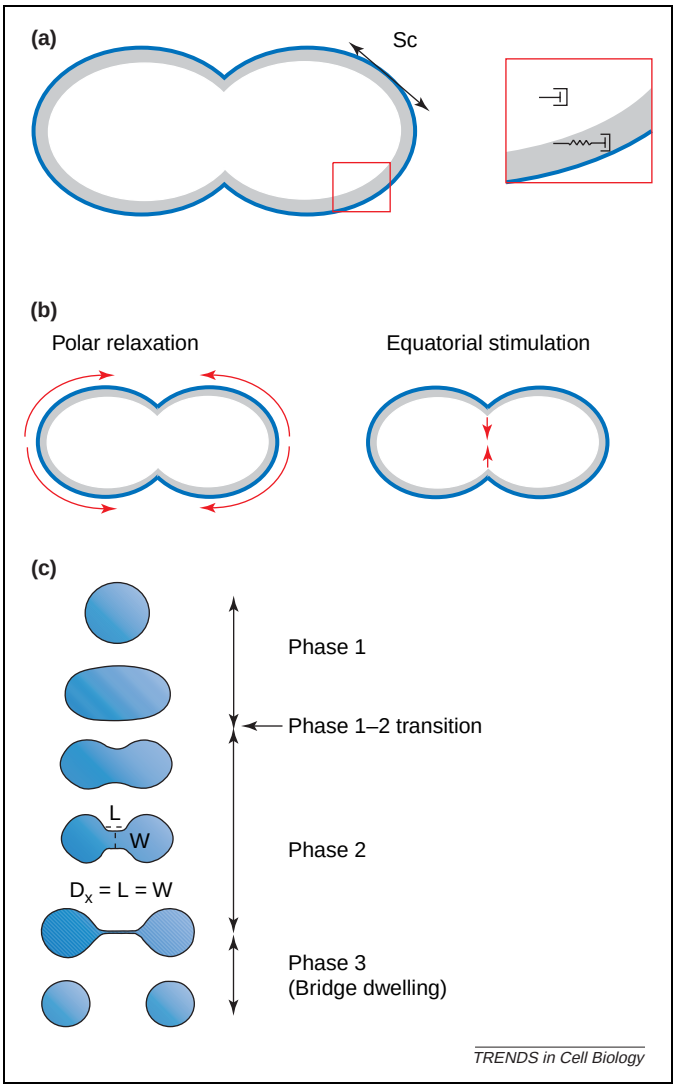

Figure 3. Models of cytokinesis. **(a)** The cortical shell–liquid core model simplifies the mechanics of the cell into a viscoelastic cortex (modeled as a spring and dashpot) that surrounds a viscous core (modeled as a dashpot). S_c denotes the stretch modulus from the in-plane elasticity of the cortex. **(b)** In the polar-relaxation model, the poles of the cell relax and their expansion drives furrow ingression. The equatorial-stimulation model attributes the principal force for cell cleavage to contraction of the equator. **(c)** During cytokinesis, cells undergo three, distinct, mechanical phases caused by the geometric and mechanical requirements of the process. Phase 1 is marked by the change from spherical to cylindrical shape and recruitment of myosin-II to the cleavage furrow. Myosin-II recruitment peaks at the phase 1–2 transition. In phase 2, the cell approaches a new equilibrium of two daughter cells. During this phase, a cylindrical bridge forms, a hallmark of which is D_x, the point at which the furrow width and length dimensions are equal. Phase 3 is distinguished by a thin bridge that connects the future daughter cells.

invoked because the cell is much larger than its individual components, thus, the material properties of the cell arise from the composite behavior of all of its molecules. Therefore, the cell is simplified to a viscoelastic cytoskeletal shell surrounding a viscous core (Figure 3a).

The cortical shell–liquid core model is a reasonable approximation for cell types such as *Dictyostelium*. In *Dictyostelium*, proteins involved in cytokinesis, including the small GTPase RacE, myosin-II, and actin crosslinkers dynacortin and cortexillin, are enriched in the cortex [8,35–38]. Perturbation of several of these proteins leads to changes in the observed stretch modulus as measured by LTM and MPA [7,17] (Table 1). However, the cortical shell–liquid core model has limitations. For example, *Dictyostelium* strains that are deficient in myosin-II do not divide in suspension but complete the process successfully on adherent surfaces. Although this indicates a role for adhesive forces during cytokinesis [39], the cortical shell–liquid core model does not readily account for adhesive forces. MPA experiments also show that the cortical shell–liquid core model does not extend to chondrocytes and endothelial cells, which behave more like solid materials [27].

Mechanics of cell division

Cell division is mechanical at almost every level. The mitotic spindle has been studied extensively for its role and the mechanism involved in driving mechanical separation of the chromosomes. Surprisingly, contraction of myosin-II in the cell cortex appears to provide additional force for centrosome separation [40]. Thus, cortical mechanics are crucial for chromosome separation, a process thought previously to involve the mitotic spindle exclusively [41].

Two classical models for cytokinesis mechanics are polar relaxation and equatorial stimulation [42–45] (Figure 3b). In the polar relaxation model, the poles of the dividing cell relax (expand), which allows ingression of the cleavage furrow. In vertebrate and *Dictyostelium* cells, Arp2/3-directed assembly of actin filaments in the polar cortex might provide a mechanism that generates force for cortex expansion [46–48]. By contrast, the equatorial-stimulation model suggests that the force required for cell division is generated from recruitment of myosin-II ATPase to the cleavage furrow. Indeed, the cleavage-furrow cortex has been shown to generate forces using glass needles and deformable substrates [49,50]. However, the genetic evidence for two pathways, global versus equatorial, indicates that these two models are extreme ends of a continuum [37]. This is supported further by studies using pharmacological inhibitors of actin such as cytochalasin D, a drug that destabilizes actin filaments. In sand dollar eggs, furrow ingression is stalled by application of cytochalasin D to the cleavage furrow, but application to the poles does not interfere with furrowing [51]. By contrast, application of cytochalasin D to the equator of dividing rat kidney cells accelerates division whereas application near the poles causes inhibition [52]. Thus, a model that includes both global and equatorial cortices that control a force-balance that governs cytokinesis dynamics is preferable. Furthermore, each side of this force-balance is established by a unique genetic program made up of distinct proteins (Table 1). In all models, asymmetry of force generation in the cell cortex is required to break the symmetry of the cell.

The shape changes of cytokinesis begin early, before anaphase. The transition from interphase to mitosis is marked by the rounding of the cell into a spherical shape as protrusive activities such as pseudopodia and lamellipodia are turned off. The Laplace pressure might drive the initial rounding of the cell in preparation for the changes in cell shape that follow. In cell types where early increases in stretch modulus have been observed, this would further facilitate rounding; however, the increase in

Table 1. Proteins involved in cytokinesis mechanics

Protein	Biochemical function	Presumed role in cytokinesis	% wild type mechanics[a]	Refs
Equatorial				
Myosin-II	Mechanochemistry	Drive equatorial constriction	70% (bending modulus, GN[b]), 30% (stretch modulus, MPA)	[16,20]
Cortexillin I,	Actin crosslinking	Focus contractile ring	70% (stretch modulus, LF, LTM), 20% (bending modulus, LF)	[7,19]
Cortexillin II	Actin crosslinking	Focus contractile ring	100% (stretch modulus, LF), 40% (bending modulus, LF)	
Cofilin	Actin-filament severing	Disassemble contractile ring	Not measured	[56]
Global				
Actin	Cytoskeletal polymer	Provide network and track	10% (stretch modulus, LTM)	[7]
RacE	Rac small GTPase	Regulate global mechanics	20% (stretch modulus, MPA)	[17]
Dynacortin	Actin crosslinking	Global mechanics	50% (stretch modulus, LTM)	[7]

[a]Mutants or latrunculin (for actin) treatment compared to wild-type, untreated control.
[b]Abbreviations: GN, glass needle; LF, laminar flow.

stiffness is apparently not (and is not predicted to be) an essential part of rounding [25]. Mobilization of cytoskeletal elements is expected to help facilitate this rounding and there are changes in cortical distribution of myosin-II during this phase [8]. Furthermore, inhibition of the Rho small GTPase disrupts these early stages of cytokinesis [53].

The spherical geometry of the rounded mother cell and the two daughter cells can be viewed as mechanical equilibrium states (Figure 3c). Thus, to pass through the shape changes of cytokinesis, the cell must move away from equilibrium before returning to equilibrium [8,54]. To move away from an equilibrium position requires work, and force production from either myosin-II or cell crawling drives this movement. One mechanical transition appears to occur when the cell becomes either oblong or cylindrical. From a simple theoretical analysis of the predicted force requirements, the maximum amount of force required correlates with the cylindrical shape [8,54]. Consistently, this cylindrical shape is the stage in which the maximum amount of myosin-II accumulates at the cleavage furrow in *Dictyostelium*. After the cylindrical-shape stage, the concentration of myosin-II in the cleavage furrow increases whereas the total amount of myosin-II in the cleavage furrow decreases. This occurs because the volume of the contractile ring decreases as furrowing progresses. The elongation from a sphere to a cylinder appears to be the phase when myosin-II is required in non-adherent *Dictyostelium* cells because *myosin-II* mutants fail to elongate during cytokinesis in suspension culture [39,55]. Thus, the adhesive forces that facilitate division in *myosin-II*-null cells must drive elongation to a cylindrical shape. We define this phase of the movement away from equilibrium as phase 1 and the cylindrical shape when the maximum amount of myosin-II accumulates as the phase 1–2 transition.

Phase 2 is the return to equilibrium as the cleavage furrow continues to constrict. During phase 2, a cylindrical bridge forms. The relative radius of the two emerging daughter cells is much larger than the radius of the cylinder, thus, the stretch modulus is predicted to energetically favor cylinder thinning because of differences in Laplace pressure between the bridge and the daughter cells [5,6] (Zhang, W.W. and Robinson, D.N. unpublished). In *myosin-II*-null cells, traction forces do not appear to be an essential part of furrowing during phase 2. If *myosin-II*-null cells simply crawl apart, then volume conservation requires that, for every 10-fold-decrease in furrow diameter, the furrow should lengthen 100-fold. In fact, *myosin-II*-mutant cells only increase their pole-to-pole distance by a small percentage during this phase. Thus, a different contractile-force generator must drive furrowing during this phase and the Laplace pressure difference is a good candidate. The traction forces might create the necessary geometry that favors a Laplace pressure that drives the remainder of furrow thinning. This Laplace pressure difference might be even stronger than predicted from a uniform stretch modulus if the stretch modulus of the furrow cortex is greater than the stretch modulus of the global cortex (as indicated by data from MPA and, possibly, AFM) [21,24–26].

Another indication of the relationship between cell mechanics and cytokinesis morphology is D_x, the point at which the cylinder length equals the cylinder width (Figure 3c). There is a linear relationship between D_x and the stretch modulus of a cell [7]. If D_x represents either a mechanical balance or transition point, then a larger restoring force provided by a stiffer global stretch modulus might resist the contractile ring, yielding a larger D_x.

A thin cylindrical bridge might persist in a dividing cell before being severed. In *Dictyostelium*, the width of the cylinder might stay at <1 μm for minutes before severing (EMR and DNR, unpublished). The thin cylindrical bridge still contains nominal amounts of actin, myosin and cross-linkers, and the time to furrow break-up is likely to be determined by disassembly of the actin network. The over-accumulation of actin observed in cleavage furrows of *Drosophila twinstar* (cofilin) mutants indicates that cofilin, a filamentous actin-severing protein, is required to disassemble the actin [56]. Many cytokinesis mutants from several organisms fail in this final stage of cytokinesis, which indicates that the dynamics of furrow break-up are crucial [57–61].

To summarize, cytokinesis includes three mechanical transitions (Figure 3c). The first mechanical transition (phase 1–2 transition) occurs when the cell is cylindrical and the maximum amount of myosin-II has accumulated in the cleavage furrow. The second mechanical transition appears to occur when D_x is achieved, and the third transition occurs when the thinned bridge has formed, which can dwell awaiting final separation [7,8,62]. This scheme allows cytokinesis mutants to be evaluated based

on which mechanical phase they arrest in (before phase 1; later, during phase 2; and near the end, before final separation of the bridge) and then related to the mechanical regime of each phase.

Concluding remarks

Cytokinesis is characterized by an elegant series of shape changes that are relatively simple geometrically. The different phases of these shape changes make it possible to consider different force-generating mechanisms and how cytoskeletal remodeling dictates these shape changes. However, to appreciate fully how proteins control shape changes of cytokinesis, the activities of each protein must be linked quantitatively to the mechanical aspects of cytokinesis. At some level, the final interpretations are connected to the model of cell mechanics that is used. Different mechanical models are better at explaining some aspects of cellular behavior than others, and none might be appropriate for every step of cytokinesis.

To understand fully how cytokinesis works, creative genetic studies coupled with quantitative dynamics analyses are required to determine how each protein contributes to furrow ingression. When deleted, many genes are likely to have a significant impact on the dynamics of cytokinesis without producing gross phenotypes. This paradox occurs because multiple force-generating mechanisms have evolved, undoubtedly for error resilience and feedback control, and to ensure that the cell can complete cytokinesis in a variety of mechanical environments. Furthermore, the material properties of the cell must also be understood because this provides the resistance to deformation during phase 1 and promotes the material forces during phase 2 of cytokinesis. However, it is not enough to understand the material properties of wild-type cells because removal of many cytokinesis proteins changes the material properties of the cell and, thus, the mechanical requirements of the mutant when it undergoes cytokinesis. Therefore, persistent integration of genetic, biochemical, biophysical and computational studies of wild-type and mutant cells are required for a sophisticated understanding of this important cell-shape change.

Acknowledgements

We thank the Robinson laboratory for comments on the manuscript, Wendy Zhang for helpful discussions, and the Burroughs Wellcome Fund, Beckman Foundation and National Institutes of Health for support to DNR and an NSF grant to P. Iglesias for JCE.

References

1 Rappaport, R. (1996) *Cytokinesis in Animal Cells*, Cambridge University Press
2 Chen, C. *et al*. (1997) Geometric control of cell life and death. *Science* 276, 1425–1428
3 Tan, J. *et al*. (2003) Cells lying on a bed of microneedles: An approach to isolate mechanical force. *Proc. Natl. Acad. Sci. U. S. A.* 100, 1484–1489
4 Vergani, L. *et al*. (2004) Modifications of chromatin structure and gene expression following induced alterations of cellular shape. *Int. J. Biochem. Cell Biol.* 36, 1447–1461
5 Zhang, W.W. and Lister, J.R. (1999) Similarity solutions for capillary pinch-off in fluids of differing viscosity. *Phys. Rev. Lett.* 83, 1151–1154
6 Entov, V.M. and Hinch, E.J. (1997) Effect of a spectrum of relaxation times on the capillary thinning of a filament of elastic liquid. *J. Non-Newtonian Fluid Mech.* 72, 31–53
7 Girard, K.D. *et al*. (2004) Dynacortin contributes to cortical viscoelasticity and helps define the shape changes of cytokinesis. *EMBO J.* 23, 1536–1546
8 Robinson, D.N. *et al*. (2002) Quantitation of the distribution and flux of myosin-II during cytokinesis. *BMC Cell Biol.* 3, 4
9 Sato, M. *et al*. (1987) Dependence of the mechanical properties of actin/α-actinin gels on deformation rate. *Nature* 325, 828–830
10 Wachsstock, D.H. *et al*. (1993) Affinity of α-actinin for actin determines the structure and mechanical properties of actin filament gels. *Biophys. J.* 65, 205–214
11 Wachsstock, D.H. *et al*. (1994) Cross-linker dynamics determine the mechanical properties of actin gels. *Biophys. J.* 66, 801–809
12 Xu, J. *et al*. (1998) Dynamic cross-linking by α-actinin determines the mechanical properties of actin filament networks. *J. Biol. Chem.* 273, 9570–9576
13 Gardel, M.L. *et al*. (2004) Elastic behavior of cross-linked and bundled actin networks. *Science* 304, 1301–1305
14 Feneberg, W. *et al*. (2001) Dictyostelium cells' cytoplasm as an active viscoplastic body. *Eur. Biophys. J.* 30, 284–294
15 Evans, E. and Yeung, A. (1989) Apparent viscosity and cortical tension of blood granulocytes determined by micropipet aspiration. *Biophys. J.* 56, 151–160
16 Dai, J. *et al*. (1999) Myosin I contributes to the generation of resting cortical tension. *Biophys. J.* 77, 1168–1176
17 Gerald, N. *et al*. (1998) A role for *Dictyostelium* racE in cortical tension and cleavage furrow progression. *J. Cell Biol.* 141, 483–492
18 Yumura, S. and Uyeda, T.Q.P. (1997) Transport of myosin II to the equatorial region without its own motor activity in mitotic *Dictyostelium* cells. *Mol. Biol. Cell* 8, 2089–2099
19 Simson, R. *et al*. (1998) Membrane bending modulus and adhesion energy of wild-type and mutant cells of *Dictyostelium* lacking talin or cortexillins. *Biophys. J.* 74, 514–522
20 Pasternak, C. *et al*. (1989) Capping of surface receptors and concomitant cortical tension are generated by conventional myosin. *Nature* 341, 549–551
21 Matzke, R. *et al*. (2001) Direct, high-resolution measurement of furrow stiffening during division of adherent cells. *Nat. Cell Biol.* 3, 607–610
22 Mijailovich, S.M. *et al*. (2002) A finite element model of cell deformation during magnetic bead twisting. *J. Appl. Physiol.* 93, 1429–1436
23 Merkel, R. *et al*. (2000) A micromechanic study of cell polarity and plasma membrane cell body coupling in *Dictyostelium*. *Biophys. J.* 79, 707–719
24 Hiramoto, Y. (1963) Mechanical properties of sea urchin eggs II. Changes in mechanical properties from fertilization to cleavage. *Exp. Cell Res.* 32, 76–89
25 Hiramoto, Y. (1990) Mechanical properties of the cortex before and during cleavage. *Ann. N. Y. Acad. Sci.* 582, 22–30
26 Wolpert, L. (1966) The mechanical properties of the membrane of the sea urchin egg during cleavage. *Exp. Cell Res.* 41, 385–396
27 Hochmuth, R.M. (2000) Micropipette aspiration of living cells. *J. Biomech.* 33, 15–22
28 Mason, T.G. *et al*. (1997) Particle tracking microrheology of complex fluids. *Phys. Rev. Lett.* 79, 3282–3285
29 McGrath, J.L. *et al*. (2000) The mechanics of F-actin microenvironments depend on the chemistry of probing surfaces. *Biophys. J.* 79, 3258–3266
30 Kuo, S.C. (2001) Using optics to measure biological forces and mechanics. *Traffic* 2, 757–763
31 Ingber, D. (2003) Tensegrity I. Cell structure and hierarchical systems biology. *J. Cell Sci.* 116, 1157–1173
32 Wang, N. and Stamenovic, D. (2000) Contribution of intermediate filaments to cell stiffness, stiffening and growth. *Am. J. Physiol. Cell Physiol.* 279, C188–C194
33 Fabry, B. *et al*. (2003) Time scale and other invariants of integrative mechanical behavior in living cells. *Phys. Rev. E Stat. Nonlin. Soft Matter Phys.* 68, 041914
34 Gunst, S.J. and Fredberg, J.J. (2003) The first three minutes: smooth muscle contraction, cytoskeletal events and soft glasses. *J. Appl. Physiol.* 95, 413–425

35 Larochelle, D.A. *et al*. (1996) A novel member of the *rho* family of small GTP-binding proteins is specifically required for cytokinesis. *J. Cell Biol.* 133, 1321–1329
36 Weber, I. *et al*. (1999) Cytokinesis mediated through the recruitment of cortexillins into the cleavage furrow. *EMBO J.* 18, 586–594
37 Robinson, D.N. and Spudich, J.A. (2000) Dynacortin, a genetic link between equatorial contractility and global shape control discovered by library complementation of a Dictyostelium discoideum cytokinesis mutant. *J. Cell Biol.* 150, 823–838
38 Moores, S.L. *et al*. (1996) Myosin dynamics in live Dictyostelium cells. *Proc. Natl. Acad. Sci. U. S. A.* 93, 443–446
39 Uyeda, T.Q.P. *et al*. (2000) Myosin II-independent cytokinesis in Dictyostelium: its mechanism and implications. *Cell Struct. Funct.* 25, 1–10
40 Rosenblatt, J. *et al*. (2004) Myosin II-dependent cortical movement is required for centrosome separation and positioning during mitotic spindle assembly. *Cell* 117, 361–372
41 Scholey, J.M. *et al*. (2003) Cell division. *Nature* 422, 746–752
42 White, J.G. and Borisy, G.G. (1983) On the mechanisms of cytokinesis in animal cells. *J. Theor. Biol.* 101, 289–316
43 Harris, A.K. and Gewalt, S.L. (1989) Simulation testing of mechanisms for inducing the formation of the contractile ring in cytokinesis. *J. Cell Biol.* 109, 2215–2223
44 Devore, J.J. *et al*. (1989) A model for astral stimulation of cytokinesis in animal cells. *J. Cell Biol.* 109, 2225–2232
45 He, X. and Dembo, M. (1997) On the mechanics of the first cleavage division of the sea urchin egg. *Exp. Cell Res.* 233, 252–273
46 Insall, R. *et al*. (2001) Dynamics of the Dictyostelium Arp2/3 complex in endocytosis, cytokinesis, and chemotaxis. *Cell Motil. Cytoskeleton* 50, 115–128
47 Cao, L-g. and Wang, Y-l. (1990) Mechanism of the formation of contractile ring in dividing cultured animal cells. I. Recruitment of preexisting actin filaments into the cleavage furrow. *J. Cell Biol.* 110, 1089–1095
48 Alsop, G.B. and Zhang, D. (2004) Microtubules continuously dictate distribution of actin filaments and positioning of cell cleavage in grasshopper spermatocytes. *J. Cell Sci.* 117, 1591–1602
49 Rappaport, R. (1967) Cell division: direct measurement of maximum tension exerted by furrow of echinoderm eggs. *Science* 156, 1241–1243
50 Burton, K. and Taylor, D.L. (1997) Traction forces of cytokinesis measured with optically modified elastic substrata. *Nature* 385, 450–454
51 Rappaport, R. (1999) Absence of furrowing activity following regional cortical tension reduction in sand dollar blastomere and fertilized egg fragment surfaces. *Dev. Growth Differ.* 41, 441–447
52 O'Connell, C.B. *et al*. (2001) Distinct roles of the equatorial and polar cortices in the cleavage of adherent cells. *Curr. Biol.* 11, 702–707
53 O'Connell, C.B. *et al*. (1999) The small GTP-binding protein rho regulates cortical activities in cultured cells during division. *J. Cell Biol.* 144, 305–313
54 Yoneda, M. and Dan, K. (1972) Tension at the surface of the dividing sea-urchin egg. *J. Exp. Biol.* 57, 575–587
55 Zang, J-H. *et al*. (1997) On the role of myosin-II in cytokinesis: division of *Dictyostelium* cells under adhesive and nonadhesive conditions. *Mol. Biol. Cell* 8, 2617–2629
56 Gunsalus, K.C. *et al*. (1995) Mutations in *twinstar*, a *Drosophila* gene encoding a cofilin/ADF homologue, results in defects in centrosome migration and cytokinesis. *J. Cell Biol.* 131, 1243–1259
57 Liu, T. *et al*. (1992) Inducible expression of calmodulin antisense RNA in *Dictyostelium* cells inhibits the completion of cytokinesis. *Mol. Biol. Cell* 3, 1403–1413
58 Tuxworth, R.I. *et al*. (1997) *Dictyostelium* RasG is required for normal motility and cytokinesis, but not growth. *J. Cell Biol.* 138, 605–614
59 Adachi, H. *et al*. (1997) *Dictyostelium* IQGAP-related protein specifically involved in the completion of cytokinesis. *J. Cell Biol.* 137, 891–898
60 Swan, K.A. *et al*. (1998) Cyk-1: a *C. elegans* FH gene required for a late step in embryonic cytokinesis. *J. Cell Sci.* 111, 2017–2027
61 Nagasaki, A. and Uyeda, T.Q. (2004) DWWA, a novel protein containing two WW domains and an IQ motif, is required for scission of the residual cytoplasmic bridge during cytokinesis in Dictyostelium. *Mol. Biol. Cell* 15, 435–446
62 Robinson, D.N. and Spudich, J.A. (2004) Mechanics and regulation of cytokinesis. *Curr. Opin. Cell Biol.* 16, 182–188
63 Heidemann, S.R. and Wirtz, D. (2004) Towards a regional approach to cell mechanics. *Trends Cell Biol.* 14, 160–166
64 Howard, J. (2001) *Mechanics of Motor Proteins and the Cytoskeleton*, Sinauer Associates